

ORIGINAL ARTICLE

Angucycline antibiotic waldiomycin recognizes common structural motif conserved in bacterial histidine kinases

Yoko Eguchi^{1,2,8}, Toshihide Okajima^{3,4,8}, Naoya Tochio^{5,6,8}, Yoichi Inukai¹, Riko Shimizu¹, Shuhei Ueda¹, Shoko Shinya¹, Takanori Kigawa⁶, Tamo Fukamizo¹, Masayuki Igarashi⁷ and Ryutaro Utsumi¹

Two-component signal transduction systems (TCSs), composed of a histidine kinase sensor (HK) and its cognate response regulator, sense and respond to environmental changes and are related to the virulence of pathogens. TCSs are potential targets for alternative antibiotics and anti-virulence agents. Here we found that waldiomycin, an angucycline antibiotic that inhibits a growth essential HK, WalK, in Gram-positive bacteria, also inhibits several class I HKs from the Gram-negative *Escherichia coli*. NMR analyses and site-directed mutagenesis studies using the osmo-sensing EnvZ, a prototypical HK of *E. coli*, showed that waldiomycin directly binds to both H-box and X-region, which are the two conserved regions in the dimerization-inducing and histidine-containing phosphotransfer (DHP) domain of HKs. Waldiomycin inhibits phosphorylation of the conserved histidine in the H-box. Analysis of waldiomycin derivatives suggests that the angucyclic ring, situated near the H-box in the waldiomycin-EnvZ DHP domain complex model, is responsible for the inhibitory activity. We demonstrate that waldiomycin is an HK inhibitor binding to the H-box region and has the potential of inhibiting a broad spectrum of HKs.

The Journal of Antibiotics (2017) 70, 251–258; doi:10.1038/ja.2016.151; published online 21 December 2016

INTRODUCTION

A search for new antibacterial targets is essential to combat the increasing development of drug resistance among bacterial pathogens. These targets are preferred to be bacteria-specific and distinct from conventional sites. Two-component signal transduction systems (TCSs) represent one of the primary means by which bacteria sense and respond to their surrounding environment. These systems are initiated by activation of histidine kinases (HKs), which situate mostly at the cell membrane and act as sensors of external environmental stimuli. On activation, a HK autophosphorylates its conserved histidine residue and then transfers the phosphate group to its cognate response regulator. In turn, the phosphorylated response regulator often controls expression of genes which contributes to cellular responses against the stimuli perceived by the HK.¹

Bacterial virulence can be considered as one form of a pathogen's adaptation to its environment and TCSs of various pathogens have been reported to be related to bacterial virulence, drug resistance or biofilm formation. Some TCSs are even involved in cell wall synthesis, cell multiplication and division, and inhibiting such systems will hinder bacterial growth.² Furthermore, TCSs are conserved in bacteria, averaging to more than 20 TCSs per species. Some TCSs are also

found in fungi and plants, but none in mammalian cells.¹ Consequently, TCS inhibitors, especially HK inhibitors, have been searched as candidates for alternative antibiotics.² Although TCSs are often studied and characterized individually, TCSs are assumed to form signal transduction networks with other TCSs within the cell. Thus, inhibiting only a single system may not be sufficient to stop the bacterial response. Inhibitors that hinder multiple signal transduction systems in a single cell could block all detours that lead to retention of virulence or survival of the bacterium.³ The catalytic regions of HKs share two highly conserved domains, the catalytic and ATP-binding (CA) domain and the dimerization-inducing His-containing phosphotransfer (DHP) domain.⁴ Inhibitors against these domains will have the potential to serve as broad-spectrum HK inhibitors.

Previous studies identified several inhibitors that block the HK CA domain. Unlike other kinases, this domain possesses an ATP-binding site, which adopts a Bergerat fold^{5–7} found in the GH1 protein family (DNA gyrase, heat shock protein 90 and DNA mismatch repair protein MutL). Radicol, an heat shock protein 90 inhibitor, interacts with residues in the ATP-binding pocket of a HK.⁶ However, binding affinity of radicol against the HK was weak compared with that against heat shock protein 90 and, consequently, radicol only showed

¹Department of Bioscience, Graduate School of Agriculture, Kindai University, Nara, Japan; ²Department of Science and Technology on Food Safety, Kindai University, Kinokawa, Japan; ³Institute of Scientific and Industrial Research, Osaka University, Ibaraki, Japan; ⁴Department of Chemistry, Osaka Medical College, Takatsuki, Japan; ⁵Research Center for the Mathematics on Chromatin Live Dynamics, Graduate School of Science, Hiroshima University, Higashi-Hiroshima, Japan; ⁶RIKEN Systems and Structural Biology Center, Yokohama, Japan and ⁷Institute of Microbial Chemistry (BIKAKEN), Tokyo, Japan

⁸These authors contributed equally to this work.

Correspondence: Dr R Utsumi, Department of Bioscience, Graduate School of Agriculture, Kindai University, 3327-204 Nakamachi, Nara 631-8505, Japan.

E-mail: utsumi@nara.kindai.ac.jp

Received 1 September 2016; revised 29 September 2016; accepted 21 November 2016; published online 21 December 2016

weak inhibition of HK activity. This suggested the possibility of GHl inhibitors as lead compounds for developing HK inhibitors.⁶ In a different study, Qin *et al.*⁸ conducted an *in silico* virtual high-throughput screen using the three-dimensional structure of the CA domain of WalK, a growth-essential HK in the low G+C, Gram-positive Firmicutes group. This screen led to the discovery of thiazolidinone derivatives that bind to the ATP-binding pocket of the WalK CA domain. However, further derivation of these compounds is necessary to reduce their animal toxicity.⁸ Small compounds binding to the ATP-binding pocket have further been searched by *in vitro* high-throughput screening or *in silico* structure-based screening.^{9–11} These studies introduce new scaffolds that could serve as starting points for designing potent HK inhibitors that interact with the ATP-binding pocket.

In a different approach, inhibitors against the growth essential WalK HK were screened from natural actinobacterial extracts by a sensitive differential growth assay.^{12–15} Among the isolated inhibitors, signermycin B inhibited WalK activity in an ATP-noncompetitive manner. Surface plasmon resonance analyses showed that signermycin B binds to the DHp domain of WalK.¹⁴ However, the mechanism of how signermycin B inhibits the WalK activity and where in the DHp domain does this inhibitor bind remain to be elucidated.

Another WalK inhibitor, waldiomycin (Supplementary Figure S1A), was also found by the sensitive differential growth assay.¹⁵ Waldiomycin is an angucycline antibiotic composed of 1, 3-dioxolane-2-carboxylic acid linked to an angucyclic polyketide via a tetraene linker and a tetrahydropyran. Its antibiotic activity is a result of its inhibition of WalK. Angucycline group antibiotics are known to have a wide range of effects as antibacterial, antiviral, anti-cancer and enzyme-inhibiting agents.¹⁶ In the present study, we employed NMR spectroscopy to elucidate that waldiomycin binds to the H-box, which comprises the autophosphorylated histidine residue and is conserved in the DHp domain of bacterial HKs. We also showed that the angucyclic polyketide moiety of waldiomycin binds adjacent to the H-box. This is the first example of a HK inhibitor binding to the H-box region and suggests the possibility of developing angucycline-based antibiotics as signal transduction inhibitors.

MATERIALS AND METHODS

HK autophosphorylation and inhibition assays

Purified HKs at a final concentration of 0.5 μM were used for autophosphorylation assay as described previously.¹⁵ Inhibition of the autophosphorylation activity of HKs was evaluated by adding drugs to the autophosphorylation reaction mixture 5 min before addition of ATP, followed by incubation at 25 °C. As for autophosphorylation of heterodimers, a mixture of 0.25 μM of EnvZ (DHp+CA) and 1 μM of EnvZ (DHp) was applied to the assay following the method essentially identical with that for homodimeric EnvZ (DHp+CA).

NMR spectroscopy

The NMR titration experiments were performed using a series of ¹H, ¹⁵N HSQC spectra in 20 mM sodium phosphate (pH 7.2), 50 mM KCl, 5 mM MgCl₂, 5 mM dithiothreitol and 10% (v/v) *d*-dimethyl sulfoxide at 288 K on a Bruker Avance II (Bruker, Billerica, MA, USA) spectrometer equipped with a triple-resonance cryogenic probe operating at 700.33 MHz for the ¹H resonance frequency. Samples containing up to 1.2 mM waldiomycin were titrated into 0.3 mM ¹⁵N-labeled EnvZ DHp domain (EnvZ (DHp)). Data processing and analysis were performed with NMRPipe¹⁷ and KUIJIRA¹⁸ running with NMRView¹⁹, respectively. The dissociation constant, K_D , was estimated to fit

equation (1)²⁰ to the bound fraction of EnvZ (DHp) dimer, f_{bound} .

$$f_{\text{bound}}([L]_{\text{total}}) = 1 - \frac{I([L]_{\text{total}})}{I_0} \\ = \frac{([P]_{\text{total}} + [L]_{\text{total}} + K_D) - \sqrt{([P]_{\text{total}} + [L]_{\text{total}} + K_D)^2 - 4[P]_{\text{total}}[L]_{\text{total}}}}{2[P]_{\text{total}}} \quad (1)$$

where $[L]_{\text{total}}$ and $[P]_{\text{total}}$ are the total concentrations of waldiomycin and EnvZ (DHp) dimer, respectively, and I and I_0 are the signal intensities with and without waldiomycin. The intensity for each signal was measured by averaging the signal intensities at the peak center and its eight surrounding points (nine-point averaging); each peak center was found by the SPARKY 'pc' function (TD Goddard and DG Kneller, SPARKY 3, University of California, San Francisco). To estimate the K_D values, we simultaneously used the buildup profiles from the signals for G240, V241, H243, N278, E282, Q283, F284, D286 and L288 for fitting in a global fitting manner. These nine residues showed severe signal reduction on the addition of 0.6 mM waldiomycin, $\text{ratio} = I(0.6)/I_0 < \text{ratio}_{\text{ave}} - \text{ratio}_{\text{std}}$, where $\text{ratio}_{\text{ave}}$ is an average value of ratios and $\text{ratio}_{\text{std}}$ is an s.d. of ratios. The uncertainty in the dissociation constant was estimated by Monte Carlo simulations on the basis of the uncertainty of each signal intensity evaluated using the root-mean-square deviation value on a spectral region with no signals, which was obtained by the NMRPipe built-in module.

The NMR samples of the wild type and mutants of the EnvZ (DHp) contained 50 or 100 μM ¹⁵N-labeled protein in 20 mM Na-phosphate (pH 7.2), 50 mM KCl, 5 mM MgCl₂, 5 mM dithiothreitol and 10% (v/v) *d*-dimethyl sulfoxide. All NMR spectra were acquired at 300 K using a Bruker Avance spectrometer equipped with a triple-resonance cryogenic probe operating at 500.13 MHz for the ¹H resonance frequency spectrometer controlled with TopSpin 3.0 software (Bruker).

Protein structure modeling

The complex model of EnvZ (DHp) with waldiomycin was constructed from the X-ray crystal structures of free EnvZ (DHp) and waldiomycin. The initial model was constructed by manually setting waldiomycin as the default based on the information from the intensity change of the NMR signals and mutagenesis experiments. The binding position of waldiomycin and its interaction were adjusted through energy minimization using the Molecular Operation Environment (Chemical Computing Group, Montreal, QC, Canada) and manual fitting. Finally, a molecular dynamics calculation was performed to remove model distortion. After the Molecular Operation Environment calculations, MMFF94x force field was selected as the default parameter set. The structure model of NtrB (GlnL) was built through homology alignment-based structure modeling by applying the *E. coli* NtrB amino acid sequence (gi: 948360) to the SWISS-MODEL web server²¹ using the coordinates of an artificial blue-light-regulated HK, YF1 (PDB entry: 4GCZ)²² as the template.

Other materials and methods including cloning, protein expression and purification, mutant constructions, chemical cross-linking, X-ray crystallography, lists of primers and plasmids are described in Supplementary Information.

RESULTS AND DISCUSSION

Waldiomycin is a general inhibitor of class I HKs

Previously, Igarashi *et al.* showed that WalK inhibitor, waldiomycin, inhibits the autophosphorylation activity of WalK HKs derived from four different species of Gram-positive bacteria, namely, *Bacillus subtilis*, *Staphylococcus aureus*, *Enterococcus faecalis* and *Streptococcus mutans*.^{15,23} We extend our analysis to ask whether waldiomycin can also inhibit HKs other than WalK. HKs can be divided into two major classes based on their domain organization, class I and class II. WalK and most of the HKs known to date are classified as class I HKs, in which the conserved phosphorylated histidine is located in the DHp domain, immediately followed by the CA domain. In class II HKs, the phosphorylated histidine is remote from the CA domain and is located in the histidine-containing

phosphotransfer domain⁴ (Supplementary Figure S1B). The cytoplasmic regions of HKs from *E. coli* and *S. mutans* were cloned, expressed and purified, and inhibitory potency of waldiomycin was evaluated. Table 1 shows the IC₅₀s of waldiomycin against the autophosphorylation activity of various HKs *in vitro*. Waldiomycin inhibited 13 out of 14 class I HKs with IC₅₀s ranging from 7.8 to 37.8 μM, suggesting that waldiomycin is a general inhibitor of class I HKs. The only exception was NtrB, with an IC₅₀ of 346 μM. In contrast, CheA, a class II HK, was resistant to waldiomycin with an IC₅₀ of 555 μM.

Waldiomycin binds to the DHP domain

The DHP and CA domains are conserved among the class I HKs. If waldiomycin targeted the CA domain, it would most likely inhibit HKs in an ATP competitive manner, as the binding of ATP is essential to the reaction. We examined inhibition of VicK, a WalK ortholog of *S. mutans*, in the presence of different concentrations of ATP. The IC₅₀s of waldiomycin against VicK in the presence of 2.5 and 100 μM ATP were 45.7 and 96.2 μM, respectively, resulting to an increase of only about twofold. On the other hand, the IC₅₀s of AMP-PNP (a nonhydrolyzable ATP analog, which inhibits HKs in an ATP competitive manner) against VicK in the presence of 2.5 and 100 μM ATP were 7.6 and 182 μM, respectively, resulting to an increase of about 24-fold. As the IC₅₀s of waldiomycin against VicK in the presence of 2.5 and 100 μM ATP did not differ as much as AMP-PNP, it was suggested that waldiomycin inhibited VicK in an ATP-noncompetitive manner. Similarly, the IC₅₀s against EnvZ, an osmosensor HK of *E. coli*, in the presence of 2.5 and 100 μM ATP were 23.9 and 23.2 μM, respectively, whereas the IC₅₀s of AMP-PNP against EnvZ in the presence of 2.5 and 100 μM ATP were 4.1 and 99.5 μM, respectively. Thus, waldiomycin also inhibited EnvZ in an ATP noncompetitive manner. These results suggest that waldiomycin is not preventing the binding of ATP to the CA domain.

To reveal the involvement of the DHP domain on the waldiomycin binding, we examined the effect of waldiomycin on dimerization of the cytoplasmic region of VicK, VicK(31–450). Addition of

waldiomycin to [γ -³²P]-phosphorylated VicK(31–450) before the glutaraldehyde treatment (for chemical cross-linking)¹⁴ prevented the dimer cross-linking and resulted in monomer-sized band in SDS-polyacrylamide gel electrophoresis, while no addition of waldiomycin mainly provided dimer-sized band (Supplementary Figure S1C, upper panel). Increasing concentration of waldiomycin further reduced the formation of the cross-linked dimer band and the monomer band of VicK(31–450) became major at over 44.5 μM waldiomycin, suggesting that waldiomycin masked the cross-linking sites or altered the distance between the cross-linking sites within the DHP domain. Furthermore, inhibition of the cross-linking correlated with the inhibition of VicK(31–450) autophosphorylation (Supplementary Figure S1C, lower panel). Waldiomycin also inhibited cross-linking within EnvZ(223–450) (DHP+CA) dimers and this correlated with the inhibition of autophosphorylation (Supplementary Figure S1D). Similar effect has been previously observed for another HK inhibitor, signermycin B, against a phosphorylated cytosolic WalK.¹⁴ Considering that the presence of the DHP domain enables HKs to exist as homodimers, it is most likely that waldiomycin inhibited HKs by binding to the DHP domain, consistent with the presumed binding site of signermycin B.

NMR and X-ray crystallographic analyses

To clarify how waldiomycin binds to the DHP domain, X-ray structural analysis of EnvZ (DHP) was first carried out, as our results showed that waldiomycin bound to EnvZ (DHP) and inhibited autophosphorylation. Despite our effort for screening, the complex structures with waldiomycin were obtained via neither co-crystallization nor soaking method for free crystals, but the free structure of EnvZ (DHP) was determined at 1.33 Å resolution (Figure 1d, Supplementary Table S3 and Supplementary Figure S5). The asymmetric unit of the solved structure contained a single peptide that is composed of two helices, helix I (R234–M258) and helix II (G264–L288), connected with a five-residue short loop. Helix I contained P248 residue where the helix kinked slightly due to lacking a hydrogen bond at the main-chain amide of P248. A four-helix bundle dimer structure was formed between two adjacent protomers that are related by crystallographic symmetry (Figure 1d).

Next, we performed NMR analyses of EnvZ (DHP) in the presence of waldiomycin to determine the binding site. ¹⁵N-labeled EnvZ (DHP) was prepared and subjected to waldiomycin titration experiments. We obtained a ¹H-¹⁵N HSQC spectra of EnvZ (DHP) and assigned the chemical shifts of the signals on the basis of the previous assignment information²⁴ that was kindly provided by Dr M Ikura (personal communication). Increasing the amount of waldiomycin in EnvZ (DHP) resulted in a reduction of signal intensities of specific signals in the ¹H-¹⁵N HSQC spectra (Figure 1a and Supplementary Figure S2A), indicating that waldiomycin binds directly to the specific sites of EnvZ in the slow exchange regime (Figure 1b). We did not observe any signals of waldiomycin in a bound form. The fraction of the waldiomycin-bound form of EnvZ (DHP) dimer was calculated with the equation (1) from the signal intensity reduction of nine residues (G240, V241 and H243 in H-box; N278, E282, Q283, F284, D286 and L288 in the helix II) that were significantly affected by adding waldiomycin. When plotted against the concentration of the EnvZ (DHP) dimer, it was found that the signal reductions were saturated when a nearly equimolar amount of waldiomycin was added (Supplementary Figure S2I). This suggests that a single waldiomycin molecule may directly interact with an EnvZ dimer. We calculated a dissociation constant of 4.34 ± 0.24 μM,

Table 1 Waldiomycin inhibits class I histidine kinases

HKs	IC ₅₀ (μM)
<i>Class I</i>	
Bs Walk	10.2 ^a
Sa Walk	8.8 ^a
Ef Walk	9.2 ^b
Sm VicK	25.8 ^b
Ec EnvZ	22.4
Ec PhoQ	12.5
Ec CpxA	12.2
Ec CreC	7.8
Ec PhoR	14.7
Ec QseC	15.1
Ec RstB	24.6
Ec YedV	14.0
Sm CiaH	37.8
Ec NtrB	346
<i>Class II</i>	
Ec CheA	555

Abbreviations: Bs, *Bacillus subtilis*; Ec, *Escherichia coli*; Ef, *Enterococcus faecalis*; Sa, *Staphylococcus aureus*; Sm, *Streptococcus mutans*.

^aThese values were adopted from Igarashi *et al.*¹⁵

^bThese values were adopted from Fakhruzaman *et al.*²²

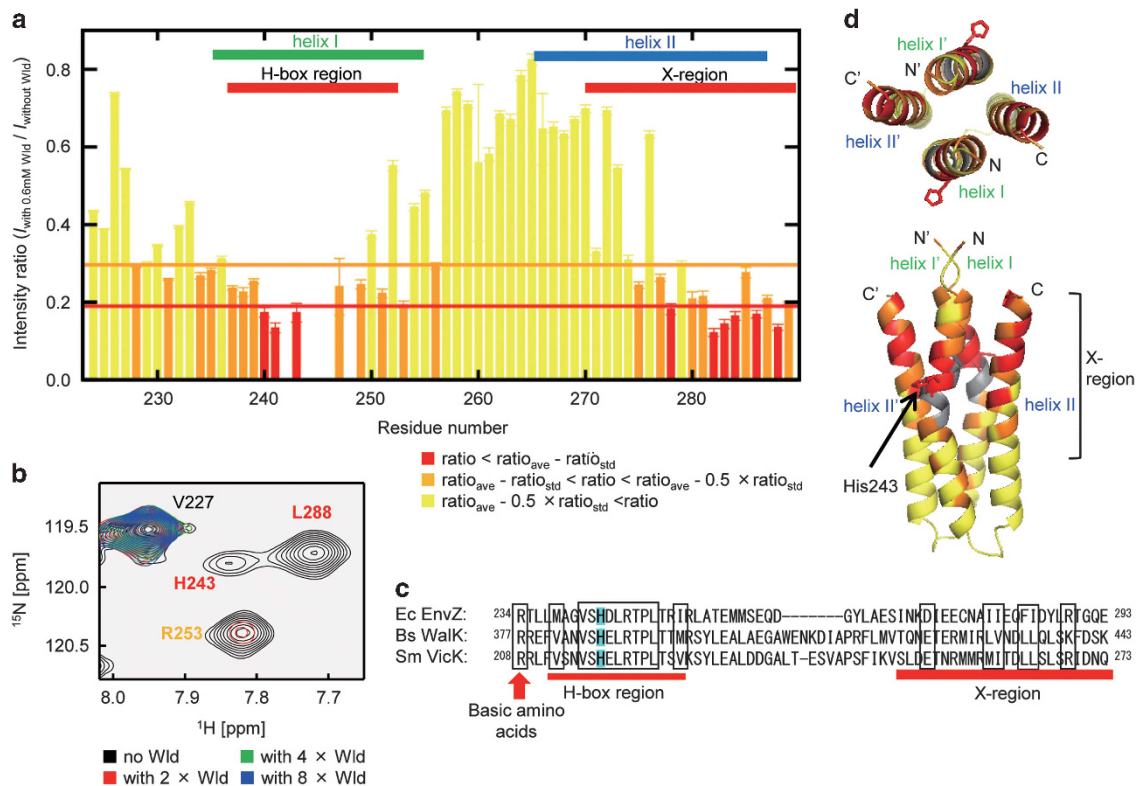


Figure 1 Waldiomycin binds to the EnvZ DHp domain at the H-box and X-regions. (a) Titration of waldiomycin into ^{15}N -labeled EnvZ (DHp). The ratio of signal intensities (ratio) in the ^1H - ^{15}N HSQC spectra between waldiomycin-treated and -untreated samples is shown. The red and orange lines indicate the values of $\text{ratio}_{\text{ave}} - \text{ratio}_{\text{std}}$ and $\text{ratio}_{\text{ave}} - 0.5 \times \text{ratio}_{\text{std}}$, respectively, where $\text{ratio}_{\text{ave}}$ and $\text{ratio}_{\text{std}}$ are the average value and the standard deviation of ratios, respectively. Amino acid residues subjected to signal reduction congregated in two regions within helices I and II. (b) ^1H - ^{15}N HSQC spectra of waldiomycin bound ^{15}N -labeled EnvZ (DHp). The [waldiomycin]/[EnvZ (DHp) dimer] ratios were 0 (black), 2 (red), 4 (green) and 8 (blue). The signal assignments were labeled and colored according to the color code in a. (c) Sequence alignment of the H-boxes and X-regions of EcEnvZ, BsWalk and SmVicK. (d) X-ray crystal structure of EnvZ (DHp) homodimer mapped with residues affected by the binding of waldiomycin. The upper figure looking down the four-helix bundle and the lower figure looking from the side of helix I.

if assumed that a single molecule of waldiomycin binds to an EnvZ dimer.

The residues that show severe signal reduction included G240-P248 in helix I and E275-R289 in helix II at the C-terminal region (Figure 1a). The former is overlapped with the H-box (L237-I252) that is a well-known conserved motif in the DHp domain of class I HKs and includes the histidine site (H243) of phosphorylation (Figure 1c). Closer examination with the E275-R289 of the helix II C-terminal region shows scattered, but significant homology with other class I HKs. This region is composed of flanking charged residues and central hydrophobic residues with moderate homology, and is designated as 'X-region' that may be important for the hydrophobic interaction between the helices.²⁵ These two regions are conserved among the class I HKs used in our study (Figure 1c and Supplementary Figure S3).

Further to elucidate the waldiomycin-binding site, residues affected by the binding of waldiomycin in our NMR analyses were mapped onto the X-ray crystal structure of the EnvZ (DHp) homodimer that was generated from the monomeric coordinates according to the crystal symmetry. As shown in Figure 1d, the affected residues of the H-box on helix I and the X-region on helix II were situated in the upper half of the homodimer. Helix I bend at P248, creating a large cleft with helix II of the identical subunit. Most of the residues that were affected by waldiomycin binding (Figure 1d) faced this cleft. In the other clefts between helices I' and II or helices I and II' (Figure 1d),

the left-faced residues in the N-terminal half of the X-region (S269, D273 and E276) showed no significant change of signal intensities upon waldiomycin binding (Figure 1a). These results suggest that waldiomycin binds to the cleft between helices I and II of the same subunit, but not to the clefts between different subunits (helices I' and II or helices I and II').

Waldiomycin inhibits autophosphorylation by binding at the H-box

Twenty nine site-directed mutant proteins of EnvZ (DHp+CA) (11 mutants in the H-box, 13 in the X-region and 5 in other region) were constructed to evaluate whether the H-box, X-region and R234 in helix I of EnvZ were critical for waldiomycin inhibitory activity. When the autophosphorylation levels of these mutants were assayed, L245A, L249A, R251A, I280A and I281A EnvZ (DHp+CA) mutants showed no or very low activity, suggesting these residues to be essential for autophosphorylation (Supplementary Figure S4A). The other mutants such as M238A, A239D, S242A, D244A, R246A, E257A, N278A, E282A, I285A, D286A, Y287A and R289A retained autophosphorylation activity (0.5–1.5-fold of the wild type; Supplementary Figure S4B) and were applied to inhibition assay with waldiomycin (Table 2). As a result, R234A and the H-box mutants, S242A, D244A, T247A and P248A, were highly resistant to waldiomycin inhibition. On the other hand, all the mutants within the X-region were sensitive to waldiomycin, suggesting that involvement

Table 2 Inhibitory effect of waldiomycin against EnvZ (DHp+CA) mutants

EnvZ (DHp+CA)	IC ₅₀ (μM)
Wild type	23.9
<i>H-box mutants</i>	
M238A	9.1
A239D	21.8
S242A	> 1420
D244A	655
R246A	12.1
T247A	338
P248A	1140
T250A	66.7
<i>X-region mutants</i>	
N278A	15.1
E282A	17.4
Q283A	48.1
F284A	84.5
I285A	8.7
D286A	33.3
Y287A	12.7
L288A	44.1
R289A	11.4
<i>Other mutations</i>	
R234A	769
T235A	45.0
R253A	10.8
E257A	15.4

The mutants in bold became resistant to waldiomycin.

of H-box and R234 of EnvZ (DHp+CA) were more important for autophosphorylation inhibition by waldiomycin.

To address whether the above mentioned mutations conferring resistance to waldiomycin affected the binding of waldiomycin to EnvZ, ¹⁵N-labeled mutant proteins of EnvZ (DHp) (S242A, D244A, T247A, P248A and R234A) were prepared and analyzed by NMR spectroscopy with increasing amount of waldiomycin. As a control, waldiomycin titration was also performed against ¹⁵N- EnvZ (DHp) E257A. This mutation conferred neither waldiomycin resistance (Table 2) nor inhibition of waldiomycin binding judged by the signal intensities and chemical shifts of the cross peaks in the ¹H-¹⁵N HSQC spectra (Supplementary Figure S2G). When waldiomycin was added to the other EnvZ (DHp) mutant proteins, the cross-peaks in the ¹H-¹⁵N HSQC spectra of S242A, D244A and P248A showed similar signal intensities and chemical shifts as those without waldiomycin. These results suggest that waldiomycin did not interact with these mutant proteins (Supplementary Figures S2B,D and F) and explain why these mutations conferred resistance against waldiomycin inhibition (Table 2). Some cross-peaks in the ¹H-¹⁵N HSQC spectra of T247A showed reduction in signal intensity by the addition of waldiomycin, but the changes were much smaller than those observed in the wild-type ¹⁵N-EnvZ (DHp) (Supplementary Figures S2A and E). This result is consistent with EnvZ (DHp+CA) T247A being less resistant to waldiomycin inhibition than the S242A, D244A and P248A mutants (Table 2). On the other hand, EnvZ (DHp) R234A showed inconsistent results. Waldiomycin binds to EnvZ (DHp) R234A judging from the reduction in signal intensities of specific cross-

peaks (Supplementary Figure S2C), although IC₅₀ of waldiomycin against EnvZ (DHp+CA) R234A is significantly increased (Table 2).

Furthermore, as for EnvZ (DHp) P248A, the X-ray crystal structure was determined to evaluate the structural change that arises from lack of the bending site of the helix I. The EnvZ (DHp) P248A structure solved at 2.23 Å contained a four-helix bundle dimer (chains A and B) in the asymmetric unit (Supplementary Table S3 and Supplementary Figures S5B and C). The structures of wild-type and P248A EnvZ (DHp) were compared by superimposing the main chain atoms of L249 – M258 of the chain A. As shown in Supplementary Figure S5C, the entire helix I of P248A EnvZ (DHp) extended in a nearly straight line, whereas that of the wild type kinked at P248. This result suggests that the structural change of the DHp domain, lying at its upper half (Supplementary Figure S5C), affected the waldiomycin-binding cleft and resulted in the significant increase of IC₅₀ for EnvZ P248A (Table 2).

Inhibitory mechanism of waldiomycin

Class I HKs generally function as homodimers. ATP first binds to the CA domain on one of the subunit and transfers the phosphate to the conserved histidine residue in the H-box of the DHp domain on the same or the other subunit. This is referred as *cis*- or *trans*-autophosphorylation.^{26,27} Whether the HK functions in a *trans* or *cis* mode is thought to be governed by the conformation of the loop at the base of the DHp domain, which connects helices I and II.²⁸ EnvZ autophosphorylates only in a *trans* manner.²⁹ Incubating EnvZ (DHp) with EnvZ (DHp+CA) at a molar ratio of 4:1 in the presence of [γ -³²P] ATP resulted in phosphorylation of both EnvZ (DHp) and EnvZ (DHp+CA) (Supplementary Figure S6B). Phosphorylation of EnvZ (DHp) in the mixed reaction is dependent on the heterodimer formation between EnvZ (DHp) and EnvZ (DHp+CA), because phosphorylation of EnvZ (DHp+CA) homodimer shows only a single phosphorylated band (Supplementary Figure S6A), whereas EnvZ (DHp) homodimer is not phosphorylated (Supplementary Figure S6C). Hence, we confirmed that EnvZ (DHp) retains the ability to accept a phosphate group from the ATP bound to the CA domain of EnvZ (DHp+CA), which is the other subunit of the heterodimer.

Waldiomycin bound to the DHp domain of EnvZ (DHp+CA) may inhibit phosphorylation of the H243 of the same subunit by masking the conserved H243 or interfering the access of the ATP-bound CA domain of the other subunit. Another possibility is that waldiomycin may block the movement of the ATP-bound CA domain by binding adjacent to the loop connecting the DHp and CA domains, and thus inhibit phosphorylation of the H243 of the other subunit. To determine how waldiomycin inhibits HK activity, we first examined whether waldiomycin is capable of inhibiting HK activity in the heterodimeric state. Waldiomycin was added to EnvZ (DHp) and EnvZ (DHp+CA) mixture, and assayed for its inhibitory activity against autophosphorylation (Figure 2a). Waldiomycin inhibited the formation of phospho-EnvZ (DHp+CA) and phospho-EnvZ (DHp) with IC₅₀s of 25.7 and 34.9 μM, respectively. When EnvZ (DHp+CA) S242A was mixed with the wild-type EnvZ (DHp) (Figure 2b), the IC₅₀s of waldiomycin against EnvZ (DHp+CA) S242A and EnvZ (DHp) were 2740 and 79.1 μM, respectively. The high IC₅₀ observed against EnvZ (DHp+CA) S242A was consistent with the results shown in Table 2 and was considered as a result from the EnvZ (DHp+CA) S242A homodimer. In contrast, the IC₅₀ of waldiomycin against EnvZ (DHp) showed only a slight increase compared to that for EnvZ (DHp) of the EnvZ (DHp)-EnvZ (DHp+CA) heterodimer (Figure 2a). Considering that waldiomycin only binds to EnvZ (DHp), and not to

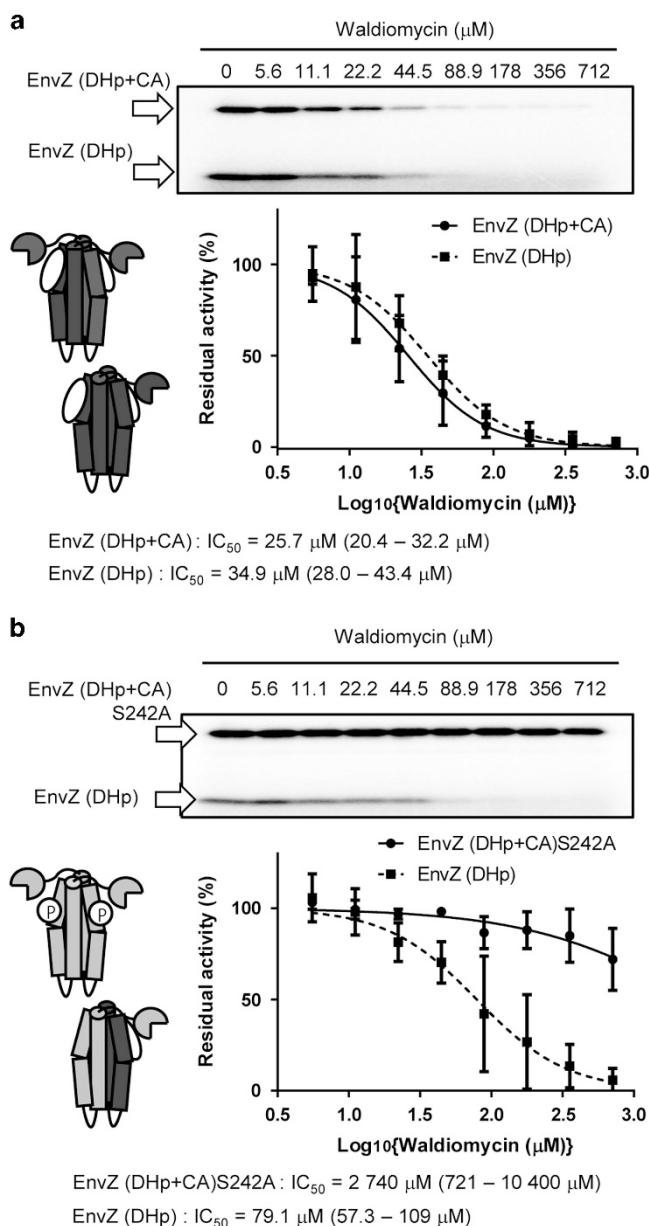


Figure 2 Waldiomycin inhibits autophosphorylation by binding to the DHp domain. Waldiomycin inhibited the phosphorylation of EnvZ (DHp+CA)-EnvZ (DHp) (a) and EnvZ (DHp+CA) S242A-EnvZ (DHp) (b) heterodimers with triplicate measurements (data represent mean \pm s.d.). EnvZ (DHp+CA) (0.25 μM) or EnvZ (DHp+CA) S242A was mixed with 1.0 μM of EnvZ (DHp) in each reaction mixture. Waldiomycin is shown as a white oval. IC_{50} s and the 95% confidence intervals shown in parenthesis were calculated by Prism 5 (GraphPad Software).

EnvZ (DHp+CA) S242A of the heterodimer, these results indicate that the binding of waldiomycin to EnvZ (DHp) inhibits the autophosphorylation of the conserved His residue of the same subunit. Taken together, we propose that waldiomycin inhibits class I HKs by binding to the H-box region and inhibits their autophosphorylation by masking this region.

Inhibitory activity of waldiomycin derivatives

To elucidate the binding mode of waldiomycin, the inhibitory activities of several waldiomycin derivatives were examined

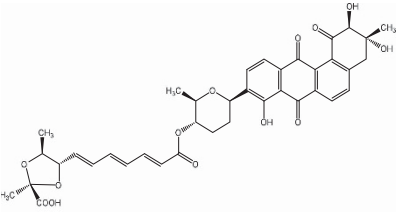
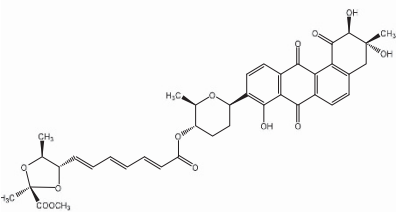
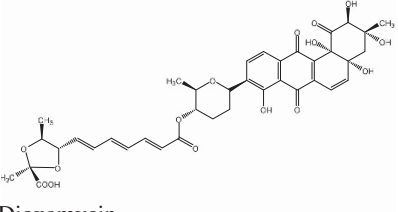
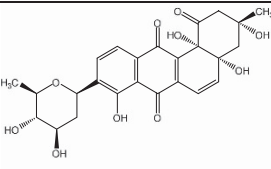
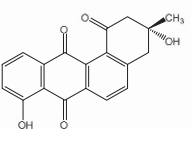
(Table 3). A methylester derivative, in which a carboxyl group in the dioxolane ring is methyl-esterified, had similar IC_{50} s for EnvZ (DHp+CA) wild type, R234A and S242A as those for waldiomycin, suggesting that the negative charge of the dioxolane ring is not likely involved in binding. This observation also suggests that conserved arginine residues of EnvZ (DHp), such as R234, R246, R251 and R289 (either occupied by arginine or lysine in class I HKs; Supplementary Figure S3), do not participate in waldiomycin binding. Dioxamycin³⁰ is another angucyclic antibiotic that is effective on Gram-positive bacteria and possesses a very similar chemical structure to waldiomycin, except that its angucyclic polyketide has two hydroxyl groups at the 4a and 12b positions. Dioxamycin also inhibits the autophosphorylation activity of EnvZ (DHp+CA), with higher potency than waldiomycin (Table 3). Introduction of the R234A or S242A mutation in EnvZ (DHp+CA) increased the IC_{50} of dioxamycin by 50–60-fold, an effect comparable with that for waldiomycin (30–60-fold increase in its IC_{50}). Aquayamycin³¹ has the same angucyclic ring as dioxamycin and tetrahydropyran, but lacks the tetraene linker and the dioxolane ring. Interestingly, aquayamycin exhibited a comparable inhibitory activity as waldiomycin for EnvZ (DHp+CA) autophosphorylation. Moreover, effect of aquayamycin on Ala mutations in the H-box region (S242, D244, T247 and P248) and R234 showed significant increase in the IC_{50} s compared with the wild type (Table 3). If the binding mode is retained among waldiomycin, dioxamycin and aquayamycin, then the angucyclic ring of these compounds should bind close to the H-box region comprising these residues. Rabelomycin³² is an antibiotic containing only the angucyclic ring moiety of waldiomycin and lacks the part spanning from the tetrahydropyran to the dioxolane ring. The IC_{50} value of rabelomycin was 14-fold higher than that of waldiomycin (Table 3). The higher IC_{50} values of aquayamycin and rabelomycin, compared with those of dioxamycin and waldiomycin, suggested that the moiety from the tetrahydropyran to the dioxolane ring contributed to the binding to EnvZ.

Modeling waldiomycin-EnvZ(DHp) complex

On the basis of the above results, waldiomycin was modeled on the X-ray crystal structure of EnvZ (DHp) (Figure 3). Considering that the cleft between helices I and II indicated large intensity changes in the cross peaks of the ^1H - ^{15}N HSQC spectra (Figure 1a) and the angucyclic ring of the bound waldiomycin was situated near the H-box, it is assumed that the dioxolane ring was bound to the X-region. This initial waldiomycin-binding model was optimized by energy-minimization and further molecular dynamic simulation. Waldiomycin was bound in a position similar to the initial model and was predicted to form several hydrogen bonds with the side chains of S242, T247, T250 and R251. Waldiomycin was fitted to the region on the cleft between helices I and II in the upper half of the four-helix bundle (Figure 3). This is the first model of a HK inhibitor binding to the DHp domain.

The dioxolane ring of waldiomycin contacts two hydrophobic residues, I285 and L288, in the X-region (Figure 3), probably through hydrophobic interactions. In agreement with the model, these residues exhibit signal reduction in the corresponding cross peaks of the ^1H - ^{15}N HSQC spectra (Figure 1a), although the changes of IC_{50} s of waldiomycin were minor for the Q283A, F284A, and L288A mutants (2.0, 3.5 and 1.8-fold increase, respectively, compared with the wild type (Table 2)). In addition to the intrinsic plasticity of the hydrophobic interactions, it is considered that the mutation to Ala results in no significant change to the hydrophobicity of the X-region. Examination of a homology model of NtrB, a class I HK with an exceptionally high IC_{50} (Table 1), also suggests the importance of the X-region. It is predicted in the NtrB model that helix II of the DHp

Table 3 Inhibitory effect of waldiomycin derivatives against EnvZ (DHP+CA) and its mutants

Drugs	IC_{50} (μM)					
	Wild type	R234A	S242A	D244A	T247A	P248A
 Waldiomycin	23.9	769	>1423	655	338	1140
 Waldiomycin methylester	27.5	116	559	ND	ND	ND
 Dioxamycin	1.36	84.2	62.8	ND	ND	ND
 Aquayamycin	14.2	224	>1030	>1030	973	>1030
 Rabelomycin	345	ND	ND	ND	ND	ND

Abbreviation: ND, not determined.

domain is short because of the inability of helix formation in the region of G187 and P188 in the X-region (Supplementary Figure S7). The model indicates that the loop region connecting the DHP and CA domains begins from G187. Superimposition of the NtrB model with the waldiomycin-bound EnvZ model suggests that the dioxolane ring moiety is located around G187 and P188. The absence of interactions with the dioxolane ring may account for the low affinity of waldiomycin toward NtrB. The NtrB model emphasizes the importance of the interaction between the X-region and the dioxolane ring.

Taken together, the results showed that waldiomycin is bound to the H-box and X-region of the DHP domain of EnvZ. The high and

moderate homology of the H-box and X-region, respectively, in class I HKs suggests that the DHP domain is the target of waldiomycin in other HKs, including WalK and VicK. The inhibitory effects of the derivatives of waldiomycin and the results from the mutation experiments indicate that the interaction between the H-box and the angucyclic ring is essential for inhibition of autophosphorylation. We conclude that waldiomycin functions as an H-box inhibitor with the potential of inhibiting a broad spectrum of HKs, suggesting the possibility of developing angucycline-based HK inhibitors.

As the orchestrated action of a number of TCSs is assumed to be involved in situations when pathogens survive in the human body and

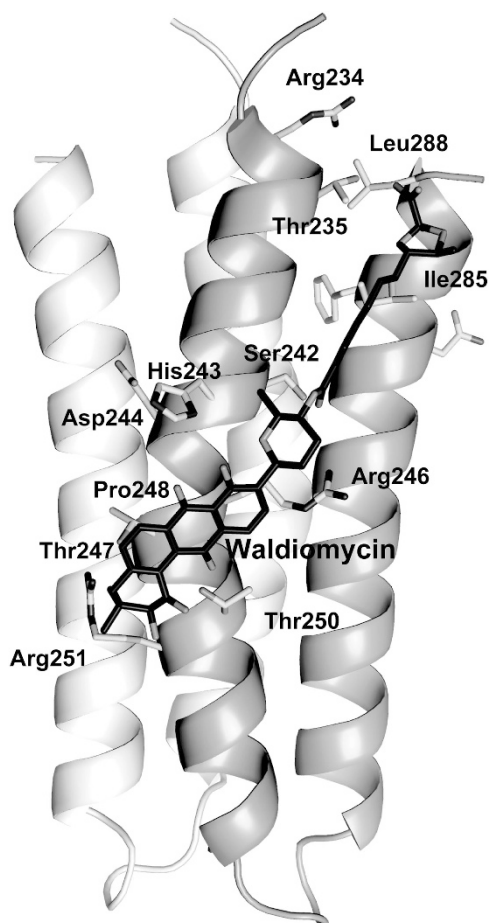


Figure 3 Model of waldiomycin bound to the EnvZ DHP domain. The complex model of EnvZ (DHP) with waldiomycin was predicted from the X-ray crystal structures of free EnvZ (DHP) and waldiomycin. Two chains forming the four-helix bundle structure are depicted by grey and light grey separately. Waldiomycin (black) and the side chain of the residues that are likely to be involved in the waldiomycin binding are shown by the stick model.

cause infectious disease, treating pathogens with broad-spectrum HK inhibitors may shut down the stress response system of bacteria, resulting in decreased viability, pathogenicity, and virulence. To date, the ATP-binding domain has been the only target for screening such HK inhibitors.^{6,8–11} With our EnvZ-waldiomycin model (Figure 3), we now propose the H-box as another promising target for obtaining broad-spectrum HK inhibitors.

CONFLICT OF INTEREST

The authors declare no conflict of interest.

ACKNOWLEDGEMENTS

We thank Dr Kiong Ho (University of Tsukuba) for the critical reading and valuable comments to the manuscript and Dr Mitsuhiro Ikura (University of Toronto) for kindly providing the signal assignment information of EnvZ (DHP). This work was supported by the Research and Development Program for New BioIndustry, Initiatives (2006–2010) of the Bio-Oriented Technology Research Advancement Institution (BRAIN), Japan (to RU), MEXT-Supported Program for the Strategic Research foundation at Private Universities, 2011–2015 (S1101035) (to RU), Platform for Dynamic Approaches to Living System (to NT) and funding from the Network Joint Research Center for Materials and Devices (to TO). This work was performed using the

synchrotron beamline station BL44XU at SPring-8 under the Cooperative Research Program of the Institute for Protein Research, Osaka University (Proposal Numbers: 2010A6511, 2010B6511, 2011A6610, 2011B6610, 2012A6710, 2013A6810, 2013B6810, 2014A6912, 2014B6912 and 2015A6508).

- 1 Stock, A. M., Robinson, V. L. & Goudreau, P. N. Two-component signal transduction. *Annu. Rev. Biochem.* **69**, 183–215 (2000).
- 2 Gotoh, Y. *et al.* Two-component signal transduction as potential drug targets in pathogenic bacteria. *Curr. Opin. Microbiol.* **13**, 232–239 (2010).
- 3 Wilke, K. E. & Calson, E. E. All signals lost. *Sci. Transl. Med.* **5**, 203ps12 (2013).
- 4 Tomomori, C., Kurokawa, H. & Ikura, M. in *Histidine Kinases in Signal Transduction* (eds Inouye, M. & Dutta, R.) 11–24 (Academic Press, San Diego, CA, USA, 2003).
- 5 Dutta, R. & Inouye, M. GHKL, an emergent ATPase/kinase superfamily. *Trends Biochem. Sci.* **25**, 24–28 (2000).
- 6 Guarnieri, M. T., Zhang, L., Shen, J. & Zhao, R. The Hsp90 inhibitor radicicol interacts with the ATP-binding pocket of bacterial sensor kinase PhoQ. *J. Mol. Biol.* **379**, 82–93 (2008).
- 7 Tanaka, T. *et al.* NMR structure of the histidine kinase domain of the *E. coli* osmosensor EnvZ. *Nature* **396**, 88–92 (1998).
- 8 Qin, Z. *et al.* Structure-based discovery of inhibitors of the YycG histidine kinase: new chemical leads to combat *Staphylococcus epidermidis* infections. *BMC Microbiol.* **6**, 96 (2006).
- 9 Cai, X. *et al.* The effect of the potential PhoQ histidine kinase inhibitors on *Shigella flexneri* virulence. *PLoS ONE* **6**, e23100 (2011).
- 10 Wilke, K. E., Francis, S. & Carlson, E. E. Inactivation of multiple bacterial histidine kinases by targeting the ATP-binding domain. *ACS Chem. Biol.* **10**, 328–335 (2015).
- 11 Velikova, N. *et al.* Putative histidine kinase inhibitors with antibacterial effect against multi-drug resistant clinical isolates identified by *in vitro* and *in silico* screens. *Sci. Rep.* **6**, 26085 (2016).
- 12 Okada, A. *et al.* Targeting two-component signal transduction: a novel drug discovery system. *Methods Enzymol.* **422**, 386–395 (2007).
- 13 Okada, A. *et al.* Walkmycin B targets WalK (YycG), a histidine kinase essential for bacterial cell growth. *J. Antibiot. (Tokyo)* **63**, 89–94 (2010).
- 14 Watanabe, T. *et al.* Isolation and characterization of signermycin B, an antibiotic that targets the dimerization domain of histidine kinase WalK. *Antimicrob. Agents Chemother.* **56**, 3657–3663 (2012).
- 15 Igarashi, M. *et al.* Waldiomycin, a novel WalK-histidine kinase inhibitor from *Streptomyces* sp MK844-mF10. *J. Antibiot. (Tokyo)* **66**, 459–464 (2013).
- 16 Rohr, J. & Thiericke, R. Angucycline group antibiotics. *Nat. Prod. Rep.* **9**, 103–137 (1992).
- 17 Delaglio, F. *et al.* NMRPipe: a multidimensional spectral processing system based on UNIX pipes. *J. Biomol. NMR* **6**, 277–293 (1995).
- 18 Kobayashi, N. *et al.* KUIRA, a package of integrated modules for systematic and interactive analysis of NMR data directed to high-throughput NMR structure studies. *J. Biomol. NMR* **39**, 31–52 (2007).
- 19 Johnson, B. A. Using NMRView to visualize and analyze the NMR spectra of macromolecules. *Methods Mol. Biol.* **278**, 313–352 (2004).
- 20 Fielding, L. NMR methods for the determination of protein-ligand dissociation constants. *Prog. Nucl. Magn. Reson. Spectrosc.* **51**, 219–242 (2007).
- 21 Biasini, M. *et al.* SWISS-MODEL: modelling protein tertiary and quaternary structure using evolutionary information. *Nucleic Acids Res.* **42**, W252–W258 (2014).
- 22 Diensthuber, R. P., Bommer, M., Gleichmann, T. & Möglich, A. Full-length structure of a sensor histidine kinase pinpoints coaxial coiled coils as signal transducers and modulators. *Structure* **21**, 1127–1136 (2013).
- 23 Fakhruzzaman, M. *et al.* Study on *in vivo* effects of bacterial histidine kinase inhibitor, Waldiomycin, in *Bacillus subtilis* and *Staphylococcus aureus*. *J. Gen. Appl. Microbiol.* **61**, 177–184 (2015).
- 24 Tomomori, C. *et al.* Solution structure of the homodimeric core domain of *Escherichia coli* histidine kinase EnvZ. *Nat. Struct. Biol.* **6**, 729–734 (1999).
- 25 Hsing, W., Russo, F. D., Bernd, K. K. & Silhavy, T. J. Mutation that alter the kinase and phosphatase activities of the two-component sensor EnvZ. *J. Bacteriol.* **180**, 4538–4546 (1998).
- 26 Dutta, R., Qin, L. & Inouye, M. Histidine kinases: diversity of domain organization. *Mol. Microbiol.* **34**, 633–640 (1999).
- 27 Casino, P., Rubio, V. & Marina, A. Structural insight into partner specificity and phosphoryl transfer in two-component signal transduction. *Cell* **139**, 325–336 (2009).
- 28 Ashenberg, O., Keating, A. E. & Laub, M. T. Helix bundle loops determine whether histidine kinases autophosphorylate in *cis* or *trans*. *J. Mol. Biol.* **425**, 1198–1209 (2013).
- 29 Yang, Y. & Inouye, M. Intermolecular complementation between two defective mutant signal-transducing receptors of *Escherichia coli*. *Proc. Natl Acad. Sci. USA* **88**, 11057–11059 (1991).
- 30 Sawa, R. *et al.* Dioxamycin, a new benz[*a*]anthraquinone antibiotic. *J. Antibiot. (Tokyo)* **44**, 396–402 (1991).
- 31 Sezaki, M., Hara, T., Ayukawa, S., Takeuchi, T. & Okami, Y. Studies on a new antibiotic pigment, aquayamycin. *J. Antibiot. (Tokyo)* **21**, 91–97 (1968).
- 32 Liu, W. C. *et al.* Isolation, characterization, and structure of rabelomycin, a new antibiotic. *J. Antibiot. (Tokyo)* **23**, 437–441 (1970).

Supplementary Information accompanies the paper on The Journal of Antibiotics website (<http://www.nature.com/ja>)